DIAS-STP-13-06

Prepared for submission to JHEP

Multi-matrix models at general coupling

Veselin G. Filev[a] **and Denjoe O'Connor**[b]

[a,b] *School of Theoretical Physics, Dublin Institute for Advanced Studies*
10 Burlington Road, Dublin 4, Ireland.

E-mail: vfilev@stp.dias.ie, denjoe@stp.dias.ie

Abstract: The eigenvalue distribution of Hoppe's two matrix model is investigated in detail as a function of the model's coupling. For small couplings it is a perturbed Wigner semicircle, while for large couplings it is a parabolic distribution which crosses over to a Wigner semicircle for eigenvalues within approximatley an inverse coupling from the boundary of the distribution. The model is approximately commuting at large couplings and we find the joint eigenvalue distribution of the two matrices. We also study a related three matrix model finding the corresponding three dimensional eigenvalue distribution there also. The techniques developed here are more widely applicable to other multi-matrix models.

Keywords: Matrix Models, 1/N Expansion

Contents

1 Introduction

Multi-matrix models play an important rôle in several branches of modern physics especially in matrix string theory [1], the IKKT model [2] (and its lower dimensional variants [3]) and the BFFS and BMN models [4, 5]. They also describe the low energy dynamics of D-branes [6] and provide simple models of emergent geometry [7, 8] and emergent gravity [9, 10].

There are very few exactly solvable interacting multi-matrix models aside from Hoppe's two matrix model [11] which we analyse in this paper. This model plays a rôle similar to that of the two dimensional Ising model in critical phenomena, being exactly solvable for many quantities while having a rich behaviour that is not easily amenable to exact analysis.

It also gives the characteristic behaviour one can expect in a wider class of multi-matrix models. The model was introduced as a guide to the physics of quantised membranes by Hoppe [11] and it has subsequently arisen in the low energy dynamics of D-branes [6] and in discussions of emergent geometry [12].

In [13] we studied the large coupling behaviour of Hoppe's model. We established that the matrices are approximately commuting at large coupling and the eigenvalue distribution of one of the matrices obeys a parabolic distribution. In an appendix we outlined the leading large coupling corrections to this parabolic distribution. We also established that the rotationally invariant 3-matrix model which reduces to Hoppe's model when one of the matrices is integrated out, has, at large coupling, a uniform joint eigenvalue distribution within a ball of radius $R \simeq \left(\frac{3\pi}{2g}\right)^{\frac{1}{3}}$ where g is the coupling of the model.

In this paper we pursue a more thorough investigation of Hoppe's model and make some further observations on its 3-matrix relative.

The principal results of this paper are:

- The eigenvalue distribution as a function of coupling, g, with perturbative expressions for large and small couplings.
- The eigenvalue density of one matrix can be "lifted" to give rotationally invariant two and three dimensional distributions, which for large g become the eigenvalue distributions for the two matrix model and its three matrix relative, respectively.
- The unique rotationally invariant "lift" to two dimensions is, for large coupling, a hemispherical distribution with a finite eigenvalue density at the boundary.
- The unique rotationally invariant "lift" to three dimensions is the uniform distribution [13], however for any finite coupling, the "lifted" distribution grows in the shell $1/g \sim r < R$ and diverges at the boundary. When reduced to the one dimensional distribution this corresponds to a crossover to the Wigner distribution as the boundary is approached.

The structure of the paper is as follows:

In section 2 we introduce Hoppe's two matrix model, expand around a background of diagonal matrices, gauge fix so that one linear combination of the matrices is diagonal. We then integrate out the all remaining modes to obtain an effective action for these longitudinal modes (eigenvalues of the diagonalised matrix). We then average over the arbitrary unit vector selecting the diagonalised matrix to get an integral equation for a rotationally invariant two dimensional distribution. We call this distribution the two dimensional "lift" of the eigenvalue distribution. The remainder of the section deals with analysing this "lifted" integral equation for weak and strong coupling. We establish that at weak coupling the solution is a uniform distribution while at strong coupling it gives a hemispherical distribution. The hemispherical lifted distribution in turn implies a parabolic eigenvalue distribution for the eigenvalue distribution of a single matrix.

Section 3 considers the one dimensional eigenvalue distribution and begins by developing perturbation theory around weak coupling. At zero coupling the eigenvalue distri-

bution is the Wigner semicircle and we show that up to order $(Rg)^6$ (where R is the extent of the distribution and g the coupling) the distribution is a Wigner semicircle modified by polynomials in $\eta = x/R$ (see equation (3.43)). Section 3.2 then develops perturbation theory for large coupling where the leading form of the distribution at large g is a parabola. An analytic form for the leading correction to the parabolic distribution is obtained. It is then shown that this reproduces the exact asymptotic growth of the observable $\nu = g^2 < \frac{\mathrm{Tr}}{N}(X^2) >$,for large g, as obtained from and exact expression found in [6].

In section 3.3 we develop a numerical technique based on the Multhopp–Kalandiya method [14] to find the eigenvalue distribution for arbitrary couplings and verify our analytic approximations for weak and strong couplings giving the regime of validity of these.

Section 4 demonstrates that given a $d-1$ dimensional distribution one can determine the rotational distribution "lifted" to d dimensions. It establishes that the uniform distribution is the "lift" of the Wigner semi-circle and that lifting the parabolic distribution with its leading correction, equation (3.43), leads to a truncated hemispherical distribution (see figure 5).

Section 5 discusses a 3 matrix variant of Hoppe's two matrix model which at large coupling was shown, [13], to have a eigenvalues uniformly distribution within a solid ball of radius $(\frac{3\pi}{2g})^{1/3}$. The integral equation for the rotationally invariant 3 dimensional "lifted" distribution is established. It is shown that quite generally the rotationally invariant $d-2$ dimensional distribution lifts to a rotationally invariant d dimensional distribution given by $\rho_d(x) = -\frac{\rho'_{d-2}(x)}{2\pi x}$. The Wigner semicircle and perturbations of it at small couplings lift to distributions that are divergent at the boundary, while the parabolic distribution lifts to the uniform distribution within a ball. The leading corrections to the parabola lifts to a distribution that is again divergent at the boundary and we establish by numerical integration of the integral equation that the characteristic behaviour for all finite couplings is the square root divergence characteristic of the "lifted" Wigner semicircle.

The paper has two technical appendices, the first, Appendix A, deals with the solution to the 2-dimensional "lifted" integral equation at large coupling while the second, Appendix B, deals with the large g asymptotics of the exact radial extent of the eigenvalue distribution $R(g)$ and the large g asymptotics of the observable ν.

2 The two-matrix model.

The principal model that we focus on in these notes is the two dimensional mass regulated model first considered by Hoppe [11]:

$$\mathcal{Z} = \int \mathcal{D}X\mathcal{D}Y e^{-N\mathrm{tr}(X^{1\,2}+X^{2\,2}-g^2[X^1,X^2]^2)} \ . \tag{2.1}$$

Our main interest is the properties of this model at strong coupling, when it is in a nearly commuting[1] phase [12]. The main strategy to solve the model is to reduce it to a one dimensional model, from which many properties can be extracted exactly.

[1] For large g we have $< \frac{Tr}{N}(i[X,Y])^2 > \simeq \frac{1}{2g^2} - \frac{1}{5g^2}(\frac{3\pi}{2g})^{2/3}$, and so X and Y commute for $g \to \infty$.

However we will first use the approach of ref. [13] and study the two matrix model directly by obtaining a two-dimensional distribution, which in the commuting phase coincides with the joint eigenvalue distribution of the matrices. To this end we split the matrices as:

$$X^1_{ij} = x^1_i \delta_{ij} + a^1_{ij}; \quad X^2_{ij} = x^2_i \delta_{ij} + a^2_{ij}; \quad \vec{x}_i = (x^1_i, x^2_i); \quad \vec{a}_{ij} = (a^1_{ij}, a^2_{ij}) \ . \tag{2.2}$$

Consider a constant unit vector $\vec{n} = (n^1, n^2)$ and define:

$$\vec{x}^{||} = \vec{n}(\vec{n}.\vec{x}); \quad \vec{x}^{\perp} = (\hat{1} - \vec{n}\vec{n}).\vec{x}; \quad \vec{a}^{||} = \vec{n}(\vec{n}.\vec{a}); \quad \vec{a}^{\perp} = (\hat{1} - \vec{n}\vec{n}).\vec{a} \ . \tag{2.3}$$

Now we can use the $SU(N)$ symmetry of the matrix model to fix the gauge:

$$\vec{n}.\vec{a}_{ij} = 0 \ . \tag{2.4}$$

After integrating out the perpendicular elements of the matrices $\vec{x}^{\perp}$ and $\vec{a}^{\perp}$ the resulting effective action for $(\vec{n}.\vec{x})$ is [13]:

$$S_{\text{eff}}[\vec{x}] = \frac{1}{N}\sum_{i=1}^{N}(\vec{n}.\vec{x}_i)^2 - \frac{1}{2N^2}\sum_{i,j=1}^{N}\log\left[\frac{(\vec{n}.(\vec{x}_i - \vec{x}_j))^2}{1 + g^2(\vec{n}.(\vec{x}_i - \vec{x}_j))^2}\right] \ . \tag{2.5}$$

Next, we consider, for large N, the continuous limit of equation (2.5) and define a rotationally invariant two dimensional distribution $\rho(\vec{x})$ so that (2.5) becomes

$$\begin{aligned} S_{\text{eff}}[\rho(\vec{x})] = &\int d^2x\rho(\vec{x})(\vec{n}.\vec{x})^2 - \frac{1}{2}\int\int d^2x d^2x'\rho(\vec{x})\rho(\vec{x}')\log\left[\frac{(\vec{n}.(\vec{x} - \vec{x}'))^2}{1 + g^2(\vec{n}.(\vec{x} - \vec{x}'))^2}\right] + \\ &+ \mu\left(\int d^2x\rho(\vec{x}) - 1\right) \ . \end{aligned} \tag{2.6}$$

Note that in general the matrices X^μ do not commute and $\rho(\vec{x})$ is a rotationally invariant "lifted" version of the one dimensional distribution of $\vec{n}.\vec{x}$. However $\vec{n}.\vec{x}$ is the eigenvalue of the matrix $\vec{n}.\vec{X}$ and when the matrices commute diagonalising $\vec{n}.\vec{X}$ would diagonalise both X^1 and X^2. Therefore for $g^2 \to \infty$ when the model is in a commuting phase $\rho(\vec{x})$ approaches the joint eigenvalue distribution of X^μ. At weak coupling the model is non-commuting and the "lifted" two dimensional distribution is a rotationally invariant lift of the eigenvalue distribution of one of the matrices, and is not itself an eigenvalue distribution.

Varying with respect ρ in equation (2.6) we obtain:

$$\mu + (\vec{n}.\vec{x})^2 = \int d^2x'\rho(\vec{x}')\log\left[\frac{(\vec{n}.(\vec{x} - \vec{x}'))^2}{1 + g^2(\vec{n}.(\vec{x} - \vec{x}'))^2}\right] \ . \tag{2.7}$$

Note that equation (2.7) should be valid for any choice of $\vec{n}$ thus in order to obtain a rotationally invariant integral equation we average over $\vec{n}$ with weight one.[2] The result is:

$$\mu + \frac{\vec{x}^2}{2} = 2\int d^2x'\rho(\vec{x}')\ln\left(\frac{|\vec{x} - \vec{x}'|}{1 + \sqrt{1 + g^2|\vec{x} - \vec{x}'|^2}}\right). \tag{2.8}$$

[2] For $\vec{n} = (\cos\phi, \sin\phi)$ we integrate both sides of the equation by $\frac{1}{2\pi}\int_0^{2\pi} d\phi$.

2.1 2D distribution at weak coupling

To obtain an integral equation suitable for perturbative calculation at small g we apply $\vec{\nabla}_x^2$ on both sides of equation (2.6). We obtain:

$$2 = \int d^2x'\,\rho(\vec{x}')\left[\vec{\nabla}_x\left(\frac{2}{\sqrt{1+g^2(\vec{x}-\vec{x}')^2}}\right).\frac{\vec{x}-\vec{x}'}{|\vec{x}-\vec{x}'|^2} + \frac{4\pi}{1+\sqrt{1+g^2|\vec{x}-\vec{x}'|^2}}\delta(\vec{x}-\vec{x}')\right]$$
$$= 4\pi\rho(\vec{x}) - 2g^2\int d^2x'\frac{\rho(\vec{x}')}{(1+g^2(\vec{x}-\vec{x}')^2)^{3/2}}\ , \tag{2.9}$$

which is an integral equation of the second kind. To avoid complications with the boundary of the integral (since the radius of the distribution runs with g) it is convenient to introduce a new variable $\vec{\eta} = \vec{x}/R$. Equation (2.9) can then be written as:

$$\rho(\vec{\eta}) = \frac{1}{2\pi} + \frac{(Rg)^2}{2\pi}\int\limits_{|\eta'|\leq 1} d^2\eta'\frac{\rho(\vec{\eta}')}{(1+(Rg)^2(\vec{\eta}-\vec{\eta}')^2)^{3/2}}\ . \tag{2.10}$$

The kernel in equation (2.10) is bounded by:

$$K_2(Rg, |\vec{\eta}-\vec{\eta}'|) \equiv \frac{1}{2\pi}\int_0^{2\pi} d\phi\frac{\eta'}{(1+(Rg)^2(\vec{\eta}-\vec{\eta}')^2)^{3/2}} \leq 1\ , \tag{2.11}$$

therefore for sufficiently small $(Rg)^2$ we can solve equation (2.10) iteratively:

$$\rho(\vec{\eta}) = \frac{1}{2\pi}\left[1 + (Rg)^2\int d^2\eta' K_2 + (Rg)^4\int d^2\eta' K_2\int d^2\eta'' K_2 + \ldots\right]\ . \tag{2.12}$$

Using equation (2.12) one can solve for $\rho(\eta)$ perturbatively to arbitrary order in (Rg). Here we present the solution to sixth order:

$$\rho(\eta) = \frac{1}{2\pi} + \frac{(Rg)^2}{4\pi} - \frac{\left(6\eta^2+1\right)(Rg)^4}{16\pi} + \frac{\left(15\eta^4+24\eta^2-2\right)(Rg)^6}{32\pi} + O\left((Rg)^8\right)\ . \tag{2.13}$$

Note that R in equation (2.13) is g dependent and expansion in g would look different. We can determine the g dependence of R using the definition of η and the normalization of $\rho(x) = \rho(\eta)$. Indeed:

$$\int d^2x\rho(x) = R^2\int d^2\eta\rho(\eta) = 1 \tag{2.14}$$

We can now substitute equation (2.13) in equation (2.14), expand R in terms of g^2 and determine the coefficients in the expansion by solving equation (2.14) order by order. This procedure can be performed to arbitrary order. Here we present the result to sixth order in g:

$$R = \sqrt{2} - \frac{1}{\sqrt{2}}g^2 + \frac{15}{4\sqrt{2}}g^4 - \frac{165}{8\sqrt{2}}g^6 + O\left(g^8\right)\ . \tag{2.15}$$

2.2 2D distribution at strong coupling

Next we focus on the large g limit of the model. It is convenient to modify equation (2.8) to:

$$\mu' + \frac{\vec{x}^2}{2} = 2\int d^2x' \rho(\vec{x'}) \ln\left(\frac{g|\vec{x} - \vec{x'}|}{1 + \sqrt{1 + g^2|\vec{x} - \vec{x'}|^2}}\right). \,, \tag{2.16}$$

where the factor of g on the right-hand side of the equation is compensated by a redefinition of the constant $\mu \to \mu'$. It is a straightforward exercise to obtain the asymptotic form of equation (2.16) in the $g \to \infty$ limit:

$$\mu' + \frac{\vec{x}^2}{2} = -\frac{2}{g}\int d^2x' \frac{\rho(\vec{x'})}{|\vec{x} - \vec{x}'|} + O\left(1/g^2\right) \,. \tag{2.17}$$

To leading order the integral equation that we obtain is:

$$\mu' + \frac{\vec{x}^2}{2} = -\frac{2}{g}\int d^2x' \frac{\rho(\vec{x'})}{|\vec{x} - \vec{x}'|} = -\frac{2}{g}\int_0^R dx' x' \int_0^{2\pi} d\phi \frac{\rho(x')}{\sqrt{x^2 + x'^2 - 2xx'\cos\phi}} \,, \tag{2.18}$$

where we have used $\rho(\vec{x}) = \rho(|\vec{x}|) = \rho(x)$. After performing the integral over ϕ we arrive at the integral equation:

$$\mu' + \frac{\vec{x}^2}{2} = -\frac{8}{g}\int_0^R dx' \frac{x'\rho(x')}{x + x'} K\left(\frac{2\sqrt{xx'}}{x + x'}\right) \,, \tag{2.19}$$

where $K(z)$ is the complete elliptic integral of the first kind. The integral equation (2.19) can be solved [15] (see also Appendix A) for $\rho(x)$:

$$\rho(x) = \frac{g}{\pi^2}\frac{\frac{1}{2}(R^2 - \mu') - x^2}{\sqrt{R^2 - x^2}} = \frac{g}{\pi^2}\sqrt{R^2 - x^2} \,, \tag{2.20}$$

where we have fixed the constant $\mu' = -R^2$ by demanding that the distribution be finite at the boundary ($x = R$). Equation (2.20) is the hemisphere distribution of ref. [12]. By normalizing the distribution $\rho(x)$ to one we can fix the radius of the distribution R:

$$R = \left(\frac{3\pi}{2g}\right)^{1/3} \,. \tag{2.21}$$

Having obtained the hemisphere distribution for $g \to \infty$ directly in two dimensions we are interested in the behaviour of the model for finite values of the coupling constant g, when the model is nearly commuting. Note that strictly speaking the correction to the joint eigenvalue distribution of the model at finite coupling is not well defined since the model is not in a commuting phase. However, there is a complex observable $\Phi = X^1 + iX^2$, which has complex eigenvalues which are well defined at any coupling. Furthermore in the commuting phase the real and imaginary components of the eigenvalues of Φ coincide with the components of the joint eigenvalues $\vec{x}$. Numerically one can simulate the model at finite g and obtain the distribution of Φ keeping in mind that in the commuting phase

this is the joint eigenvalue distribution. In order to compare to numerical simulations we need to understand the behaviour of the distribution for large but finite g.

It turns out that it is technically easier to determine the correction to the hemisphere distribution by integrating out one of the matrices and study the corresponding one dimensional distribution. In the next section we analyze the reduced model and the one dimensional distribution at general coupling g. As we show by solving an integral equation of Abel's type we can lift the one dimensional distribution to a rotationally invariant two dimensional one.

3 The one matrix model

In this section we focus on the one-dimensional distribution of the matrix $\vec{n}.\vec{X}$ defined in the previous section. Without loss of generality we can choose $\vec{n} = (1, 0)$ and $\vec{x} = (x, y)$. The integral equation for the distribution $\rho_1(x)$ is given by:

$$\mu' + x^2 = \int dx' \rho_1(x') \log \left[\frac{g^2(x - x')^2}{1 + g^2(x - x')^2} \right] , \tag{3.1}$$

where we have substituted the definition of $\rho_1(x)$:

$$\rho_1(x) = \int_{-\sqrt{R^2-x^2}}^{\sqrt{R^2-x^2}} \rho(\sqrt{x^2 + y^2}) dy . \tag{3.2}$$

in equation (2.7) and have redefined the constant $\mu \to \mu'$ to add the factor of g^2 in the argument of the logarithmic function in equation (3.1). It is convenient to differentiate equation (3.1) with respect to x. The resulting integral equation can be written as:

$$-x = \int_{-R}^{R} dx' \frac{\rho_1(x')}{x' - x} + \int_{-R}^{R} dx' \rho_1(x') K(g, x' - x) , \tag{3.3}$$

where the kernel $K(g, u)$ is given by:

$$K(g, u) = -\frac{g^2 u}{1 + g^2 u^2} . \tag{3.4}$$

3.1 1D distribution at weak coupling

At $g = 0$ we have $K(0, u) = 0$ and the integral equation (3.3) has a simple Cauchy kernel:

$$-x = \int_{-R}^{R} dx' \frac{\rho_1(x')}{x' - x} . \tag{3.5}$$

Note that at vanishing coupling the model is Gaussian and hence the one dimensional distribution of X^1, or equivalently $\vec{n}.\vec{X}$, should be a Wigner semi-circle. The unique bounded solution of equation (3.5) is indeed the Wigner semicircle (3.6).

$$\rho_1(x) = \frac{1}{\pi} \sqrt{R^2 - x^2} , \tag{3.6}$$

with radius $R = \sqrt{2}$, which agrees with the $Rg \to 0$ limit of equation (2.15). The perturbative solution for small g can be obtained, in terms of the coordinate $\eta = x/R$ and the coupling Rg, by integrating out one of the components of $\vec{\eta}$ in equation (2.13) :

$$\tilde{\rho}(\eta_1) = \int_{-\sqrt{1-\eta_1^2}}^{\sqrt{1-\eta_1^2}} \rho(\sqrt{\eta_1^2 + \eta_2^2})\, d\eta_2 \quad , \tag{3.7}$$

where $\tilde{\rho}(\eta)$ is related to $\rho_1(x)$ via:

$$\tilde{\rho}(\eta) = \frac{1}{R}\rho_1(R\,\eta) \ . \tag{3.8}$$

The final expression for small Rg up to sixth order is given by:

$$\rho_1(\eta) = \sqrt{1-\eta^2}\left[\frac{1}{\pi} + \frac{(Rg)^2}{2\pi} - \frac{\left(4\eta^2+3\right)(Rg)^4}{8\pi} + \frac{\left(8\eta^4+20\eta^2+9\right)(Rg)^6}{16\pi} + O\left((Rg)^8\right)\right] . \tag{3.9}$$

As one can see, the small Rg corrections deform the Wigner semicircle but it still has the characteristic $\sqrt{1-\eta^2}$ behaviour.

3.2 1D distribution at strong coupling

For large g one can use:

$$\frac{1}{u} + K(g,u) = -\frac{\pi}{g}\delta'(u) + O\left(1/g^2\right) \tag{3.10}$$

to obtain:

$$-x = \frac{\pi}{g}\rho_1(x) + O\left(1/g^2\right) \ , \tag{3.11}$$

which to leading order in g is solved by the parabolic distribution [12]:

$$\rho_1(x) = \frac{3}{4R^3}(R^2 - x^2) = \frac{g}{2\pi}(R^2 - x^2) \ . \tag{3.12}$$

with radius given by equation (2.21).

In order to obtain the corrections to the parabolic distribution at finite g we will derive an integral equation of the second kind which can (at least in principal) be solved iteratively. Let us begin by noting that the kernel of the integral equation (3.3) can be written as:

$$\frac{1}{x'-x} + K(g, x'-x) = \frac{d}{dx'}K_1(g, x'-x) \ , \tag{3.13}$$

where $K_1(g, x'-x)$ is the symmetric kernel:

$$K_1(g, x'-x) = \frac{1}{2}\log\left[\frac{g^2(x-x')^2}{1+g^2(x-x')^2}\right] \ . \tag{3.14}$$

After integration by parts, and noting that $\rho(\pm R) = 0$, equation (3.3) can be written as:

$$x = \int_{-R}^{R} dx'\, K_1(g, x'-x)\, \rho_1'(x') \ . \tag{3.15}$$

Again, to deal with the g dependence of the limits of the integral, it is convenient to rewrite the integral equation (3.15) in terms of the variables $\eta = x/R$, Rg and the distribution $\tilde{\rho}(\eta) = \frac{\rho_1}{R}$ so that (3.15) becomes:

$$\eta = \int_{-1}^{1} d\eta' \, K_1(Rg, \eta' - \eta) \, \tilde{\rho}'(\eta') \ . \tag{3.16}$$

At large Rg the kernel K_1 has the expansion:

$$K_1 = -\frac{\pi}{Rg}\delta(\eta' - \eta) + O\left(1/(Rg)^2\right) \ . \tag{3.17}$$

Next we define the kernel:

$$\Delta K(Rg, \eta' - \eta) = -\frac{Rg}{\pi} K_1(Rg, \eta' - \eta) - \delta(\eta' - \eta) \tag{3.18}$$

with $\Delta\tilde{\rho}$ defined by:

$$\Delta\tilde{\rho}'(\eta) = \tilde{\rho}'(\eta) - Rg\,\tilde{\rho}_{(0)}(\eta) = \tilde{\rho}'(\eta) + \frac{Rg}{\pi}\,\eta \ , \tag{3.19}$$

where $\tilde{\rho}_{(0)}$, given by:

$$\tilde{\rho}_0(\eta) = \frac{1}{2\pi}(1 - \eta^2), \tag{3.20}$$

is the parabolic distribution (3.12) valid in the strict $g \to \infty$ ($Rg \to \infty$) limit. The integral equation (3.16) can be written as:

$$\Delta\tilde{\rho}'(\eta) = -Rg \int_{-1}^{1} d\eta' \, \Delta K(Rg, \eta' - \eta) \, \tilde{\rho}'_{(0)}(\eta') - \int_{-1}^{1} d\eta' \, \Delta K(Rg, \eta' - \eta) \, \tilde{\Delta}\rho'(\eta') \ . \tag{3.21}$$

Equation (3.21) is an integral equation of the second kind for the correction $\Delta\tilde{\rho}$. Furthermore, from the definition of ΔK and the expansion of K_1 at large Rg, equation (3.17), it follows that ΔK dies out at large Rg and hence the integral equation (3.21) can be developed recursively in a convergent series:

$$\Delta\tilde{\rho}'(\eta) = -Rg \int \Delta K \, \tilde{\rho}'_{(0)} + Rg \int \Delta K \int \Delta K \, \tilde{\rho}'_{(0)} - Rg \int \Delta K \int \Delta K \int \Delta K \, \tilde{\rho}'_{(0)} + \dots \ . \tag{3.22}$$

If we define $\tilde{\rho}'_{(1)}(Rg, \eta) = -Rg \int \Delta K \, \tilde{\rho}'_{(0)}$ and:

$$\tilde{\rho}'_{(n+1)}(Rg, \eta) = -\int_{-1}^{1} d\eta \, \Delta K(Rg, \eta' - \eta) \, \tilde{\rho}'_{(n)}(Rg, \eta') \quad n = 1, 2, \dots \ , \tag{3.23}$$

we arrive at the following expression for $\Delta\tilde{\rho}(\eta)$:

$$\Delta\tilde{\rho}(\eta) = \sum_{n=1}^{\infty} \int_{-1}^{\eta} d\eta' \, \frac{\tilde{\rho}'_{(n)}(Rg, \eta')}{(Rg)^{n-1}} \ . \tag{3.24}$$

At large Rg we have $1/Rg < \int \Delta K < 1$. Therefore:

$$\frac{1}{(Rg)^{n-1}} < \frac{\tilde{\rho}'_{(n)}(Rg,\eta)}{(Rg)^{n-1}} < \frac{1}{(Rg)^{n-2}} \tag{3.25}$$

and naively one would expect that at large Rg the contribution to $\Delta\tilde{\rho}$ in equation (3.24) from terms with $n > 1$ would die out. However one can show that $\tilde{\rho}'_{(n)}(\infty,\eta)$ is not integrable near the boundary ($\eta = \pm 1$) and by regulating it with a cutoff of the order $\sim 1/(Rg)$ one can estimate that for large Rg: $\int \tilde{\rho}'_{(n)}(Rg,\eta) \sim (Rg)^{n-1}$ for $n > 1$ and $\int \tilde{\rho}'_{(1)}(Rg,\eta) \sim \log(Rg)$ for $n = 1$. Therefore for $n > 1$ we have that $\tilde{\rho}'_{(n)}(Rg,\eta)/(Rg)^{n-1} \sim [\delta(1-\eta) - \delta(1+\eta)]$ for sufficiently large Rg and all terms with $n > 1$ give a constant contribution $\kappa \sim 1$ to $\Delta\tilde{\rho}$ in equation (3.24) as long as $\eta \in (-1,1)$. At the boundary the contribution from all terms vanishes and we have $\Delta\tilde{\rho}(\pm 1) = 0$. Therefore to leading order we have the following expression for $\Delta\tilde{\rho}$:

$$\Delta\tilde{\rho}(\eta) = \begin{cases} \int_{-1}^{\eta} d\eta' \tilde{\rho}'_{(1)}(Rg,\eta') + \kappa + O((\log(Rg)/Rg) & \text{if } -1 \le \eta \le 1 \\ 0 & \text{if } \eta = \pm 1 \end{cases} \tag{3.26}$$

Using the definitions from equations (3.20) and (3.23) we can obtain the following expression for $\tilde{\rho}'_{(1)}$:

$$\begin{aligned} \tilde{\rho}'_{(1)}(Rg,\eta) = & \frac{Rg\,\eta}{\pi^2}\left[\tan^{-1}[Rg(1+\eta)] + \tan^{-1}[Rg(1-\eta)] - \pi\right] + \frac{1}{4\pi^2}\log\left[\frac{1+(Rg)^2(1-\eta)^2}{1+(Rg)^2(1+\eta)^2}\right] \\ & + \frac{(Rg)^2}{4\pi^2}(1-\eta^2)\log\left[\frac{(1+\eta)^2(1+(Rg)^2(1-\eta)^2)}{(1-\eta)^2(1+(Rg)^2(1+\eta)^2)}\right] . \end{aligned} \tag{3.27}$$

Note that:

$$\tilde{\rho}'_{(1)}(\infty,\eta) = -\frac{1}{\pi^2}\frac{\eta}{1-\eta^2} + \frac{1}{2\pi^2}\log\left[\frac{1-\eta}{1+\eta}\right] , \tag{3.28}$$

which is indeed not integrable near $\eta = \pm 1$. Let us introduce a cutoff ϵ. The regulated expression for $\tilde{\rho}_{(1)}$ is:

$$\tilde{\rho}^{(\epsilon)}_{(1)}(\eta) = \frac{1}{2\pi^2}\,\eta\,\log\left[\frac{1-\eta}{1+\eta}\right] + \frac{1}{2\pi^2}\log\left[\frac{2}{\epsilon}\right] + O\left(\epsilon\,\log(\epsilon)\right) . \tag{3.29}$$

The cutoff ϵ can be expressed in terms of Rg. Indeed if we integrate directly the integrable expression (3.27) we obtain:

$$\tilde{\rho}_{(1)}(Rg,\eta) = \frac{Rg}{2\pi}\left[T_1(Rg,\eta) + T_2(Rg,\eta) + T_3(Rg,\eta)\right] , \tag{3.30}$$

where T_1, T_2 and T_3 are given by:

$$\begin{aligned} T_1(Rg,\eta) = (1-\eta^2)\left(1 - \frac{\tan^{-1}(Rg(1-\eta)) + \tan^{-1}(Rg(1+\eta))}{\pi}\right) \\ + \frac{\tan^{-1}(2Rg) - \tan^{-1}(Rg(1+\eta)) - \tan^{-1}(Rg(1-\eta))}{3\pi\,(Rg)2} , \end{aligned} \tag{3.31}$$

$$T_2(Rg,\eta) = \frac{1}{2\pi\, Rg}\left(\eta\,\log\left[\frac{1+(Rg)^2(1-\eta)^2}{1+(Rg)^2(1+\eta)^2}\right] + \log(1+4(Rg)^2)\right)\,, \tag{3.32}$$

$$\begin{aligned} T_3(Rg,\eta) = {} & \frac{Rg}{3\pi}\log\left[\frac{(Rg)^4(1-\eta^2)^2}{(1+(Rg)^2(1-\eta)^2)(1+(Rg)^2(1+\eta)^2)}\right] \\ & - \frac{Rg}{2\pi}\,\eta\left(1-\frac{\eta^2}{3}\right)\log\left[\frac{(1-\eta)^2(1+(Rg)^2(1+\eta)^2)}{(1+\eta)^2(1+(Rg)^2(1-\eta)^2)}\right] \\ & - \frac{2Rg}{3\pi}\log\left[\frac{4(Rg)^2}{1+4(Rg)^2}\right]\,. \end{aligned} \tag{3.33}$$

For the large Rg expansion of $\tilde{\rho}_{(1)}$ we obtain:

$$\tilde{\rho}_{(1)}(Rg,\eta) = \frac{1}{2\pi^2}\,\eta\,\log\left[\frac{1-\eta}{1+\eta}\right] + \frac{1}{2\pi^2}\,\log(2\,e^{3/2}\,Rg) + O(\log(Rg)/(Rg))\,. \tag{3.34}$$

Comparing equations (3.29) and (3.34) we conclude that $\epsilon = e^{-3/2}/(Rg) \sim 1/(Rg)$, which agrees with the analysis performed below equation (3.25). Taking into account the constant κ from equation (3.26) we arrive at the following expression for $\tilde{\rho}$ in the interval $\eta \in (-1,1)$:

$$\tilde{\rho}(\eta) = \frac{Rg}{2\pi}\,\left(1-\eta^2\right) + \frac{1}{2\pi^2}\,\eta\,\log\left[\frac{1-\eta}{1+\eta}\right] + \frac{1}{2\pi^2}\,\log(2\,e^{3/2}\,Rg) + \kappa + O(\log(Rg)/(Rg))\,. \tag{3.35}$$

Note that at large Rg the correction, $\Delta\tilde{\rho}$, vanishes at $\eta = 1-\delta_1$, where to leading order $\delta_1 = \frac{W(-3/2-2\pi^2\kappa)}{2\,\pi\,Rg}$ and $W(z)$ is the Lambert's product log function — the solution to $z = W(z)e^{W(z)}$. Therefore, at large Rg, to a very good approximation $\Delta\tilde{\rho}(\eta)$ is given by equation (3.35) in the interval $\eta \in (-1+\delta_1, 1-\delta_1)$ and can be taken as zero outside this interval.

The constant κ in equation (3.35) can be determined numerically by computing $\tilde{\rho}_{(n)}$ up to sufficiently large n. However one can also fix κ indirectly by comparing to some of the exact relations for the observables of this model. Indeed, following the approach of ref. [6] one can obtain an exact relation between the radius of the distribution and the coupling constant g. This relation is rather complex and is given parametrically in terms of elliptic integrals. For a more detailed derivation we refer the reader to appendix B. Here we provide only the first few terms in the large g expansion of R.

$$R = \left(\frac{3\pi}{2}\right)^{1/3} g^{-1/3} - \frac{2\log\,g + \log(96\pi^4)}{6\pi} g^{-1} + O(g^{-5/3})\,. \tag{3.36}$$

The radius of the distribution R can also be calculated using that:

$$\frac{1}{R^2} = \int_{-1}^{1} d\,\eta\,\tilde{\rho}(\eta) = \frac{Rg}{2\pi}\int_{-1}^{1} d\eta\,(1-\eta^2) + \int_{-1}^{1} d\eta\,\Delta\tilde{\rho}(\eta)\,. \tag{3.37}$$

Substituting the expression for $\Delta\tilde{\rho}$ from equation (3.35) into equation (3.37) and solving for R order by order in g one arrives at:

$$R = \left(\frac{3\pi}{2}\right)^{1/3} g^{-1/3} - \frac{4\log\,g + 2\log(12\pi) + 12\pi^2\,\kappa + 3}{12\pi} g^{-1} + O(g^{-5/3})\,. \tag{3.38}$$

Comparing equations (3.36) and (3.38) we obtain:

$$\kappa = \frac{\log(4\pi^2) - 1}{4\pi^2} \ . \tag{3.39}$$

and we find the correction $\Delta\tilde{\rho}$ is given by:

$$\Delta\tilde{\rho}(\eta) = \frac{1}{2\pi^2}\,\eta\,\log\left[\frac{1-\eta}{1+\eta}\right] + \frac{\log(4\pi\,Rg)+1}{2\pi^2} + O\left(\frac{\log(Rg)}{Rg}\right) \tag{3.40}$$

and our expression for the $\tilde{\rho}(\eta)$ in the large Rg regime is

$$\tilde{\rho}(\eta) \simeq \begin{cases} \frac{Rg}{2\pi}(1-\eta^2) + \frac{1}{2\pi^2}\,\eta\,\log\left[\frac{1-\eta}{1+\eta}\right] + \frac{\log(4\pi\,Rg)+1}{2\pi^2} + O\left(\frac{\log(Rg)}{Rg}\right) & \text{if } |\eta| \le 1-\delta \\ 0 & \text{if } |\eta| \ge 1-\delta \end{cases} , \tag{3.41}$$

where $\delta = W(1/e)/(2\pi Rg) \sim 1/Rg$ and $W(z)$ is the Lambert's product log function.

Our expression for the leading correction to the distribution can be tested by calculating the observable $\nu = g^2 < TrX^2 >$, which was obtained in closed form in ref. [6] (see also appendix B). Indeed from the definition of ν and $\tilde{\rho}(\eta)$ it follows that:

$$\nu = g^2 \int_{-R}^{R} dx\, x^2 \rho_1(x) = R^2 (Rg)^2 \int_{-1}^{1} d\eta \eta^2 \tilde{\rho}(\eta) = \frac{(12\pi)^{2/3}}{20} g^{4/3} - \frac{3}{(12\pi)^{2/3}} g^{2/3} + O(g^0) \ , \tag{3.42}$$

which is in perfect agreement with the result of ref. [6]. In deriving (3.42) we have used equations (3.36) and (3.41).

Finally let is obtain the leading order behavior of $\rho_1(x)$ at large g. Using $\rho_1(x) = R\tilde{\rho}(x/R)$ and equations (3.36) and (3.41) we obtain:

$$\rho_1(x) = \frac{g}{2\pi}\left[\left(\frac{3\pi}{2g}\right)^{2/3} - x^2\right] + \frac{x}{2\pi^2}\log\left[\frac{\left(\frac{3\pi}{2g}\right)^{1/3} - x}{\left(\frac{3\pi}{2g}\right)^{1/3} + x}\right] + \frac{1}{2\pi^2}\left(\frac{3\pi}{2g}\right)^{1/3} + O\left(\frac{\log g}{g}\right) \tag{3.43}$$

In the next subsection we develop a numerical routine to obtain the one dimensional distribution for arbitrary values of the coupling (Rg).

3.3 Interpolating solution for general coupling.

In this subsection we construct an interpolating solution to the integral equation:

$$-\eta = \int_{-1}^{1} d\eta' \,\frac{\tilde{\rho}(\eta')}{\eta' - \eta} + \int_{-1}^{1} d\eta'\,\tilde{\rho}(\eta')\,K(Rg, \eta' - \eta) \ , \tag{3.44}$$

where K is defined in equation (3.4). Equation (3.44) is a singular integral equation of the first kind with a Cauchy kernel. An interpolating solution of this equation can be found using the Multhopp–Kalandiya method (see ref.[14] Chapter 14.5). When the source is odd

($-\eta$ in our case) the approximate solution bounded at the boundary of the distribution ($\eta = \pm 1$) is given by:

$$\tilde{\rho}_a(\cos\theta) = \frac{4}{\pi(2n+1)} \sum_{l=1}^{n} \tilde{\rho}(\cos\theta_l) \frac{\cos\left(\frac{l\pi}{2n+1}\right) \sin\left(\frac{n\,l\,\pi}{2n+1}\right) \sin((2n+1)\theta)}{\cos(2\theta) - \cos\left(\frac{2l\pi}{2n+1}\right)}, \tag{3.45}$$

where $\cos\theta = \eta$, $2n$ is the number of nodes into which the interval $[-1, 1]$ is divided and θ_l are related to the roots of the Chebyshev polynomial of the second kind:

$$\eta_l = \cos\theta_l, \quad \theta_l = \frac{l\pi}{2n+1}\ , \quad l = 1, \ldots, 2n\ . \tag{3.46}$$

The value of $\tilde{\rho}$ at the nodes η_l is determined by the system of linear algebraic equations:

$$\sum_{l=1}^{n} (c_{k,l} - c_{2n+1-k,l}) \tilde{\rho}(\cos\theta_l) = -\cos\theta_k, \quad k = 1, \ldots\ n\ , \tag{3.47}$$

where

$$c_{kl} = \frac{\sin\theta_l}{2n+1} \left[\frac{2\epsilon_{kl}}{\cos\theta_l - \cos\theta_k} + K(Rg, \cos\theta_k, \cos\theta_l) \right] \text{ and } \epsilon_{lk} = (k-l) \mod 2\ . \tag{3.48}$$

By choosing sufficiently large n one can generate numerical solution of almost arbitrary precision. Using:

$$R = \left[\int_{-1}^{1} d\eta\, \tilde{\rho}(\eta) \right]^{-\frac{1}{2}} \quad \text{and} \quad \rho_1(x) = R\, \tilde{\rho}(x/R)\ , \tag{3.49}$$

one can generate an approximate numerical solution for $\rho_1(x)$. In figure 1 we present the plot of the distribution $\rho_1(x)$ for range of coupling constants $0 \leq g \leq 133.3$. The black dashed curve in the figure represents the Wigner semi-circle (3.6) one can see the perfect fit with the data for $g = 0$. The red dashed curve fits the curve for the highest value of g ($g = 133.3$) and represents the analytic expression for the distribution at large g given in equation (3.43). One can see the excellent agreement of the numerical results with the analytic analysis from the previous subsection.

Let us now verify the approximate solutions for $\tilde{\rho}(\eta)$ obtained in the previous section. In figure 2 we have presented plots of $\tilde{\rho}(\eta)$ for small values of the coupling constant $0 \leq Rg \leq 0.6$. The dashed red curves in figure 2 represent the approximate solution for small Rg from equation (3.9) while the blue ones are the numerical solution. One can see that the approximation is excellent for $Rg < 0.6$ and is reasonably good for $Rg = 0.6$.

Next we focus on the large Rg regime. In figure 3 we present plots of $\tilde{\rho}(\eta)$ for $3 \leq Rg \leq 18$. The dashed red curves represent $\tilde{\rho}(\eta)$ given in equation (3.41). One can see how the approximation improves as we increase Rg and at $Rg = 18$ it is already excellent.

To further verify the correctness of our numerical approach we evaluate some of the observables of the model which can be obtained in closed form [6] (see also appendix B). In figure 4 we present plots of the radius of the distribution and the observable ν (defined in equation (B.2)) as a function of the coupling constant g.

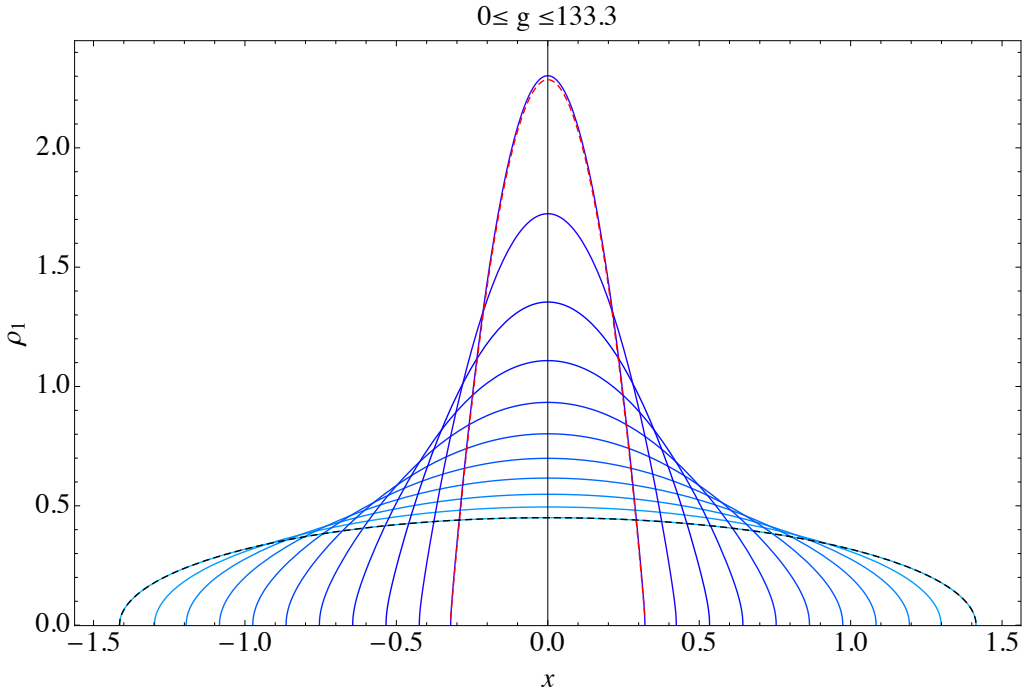

Figure 1. The eigenvalue density $\rho_1(x)$ for small coupling $0 \leq g \leq 133.3$. The black dashed curve is the Wigner semi-circle ($g = 0$) while the red dashed curve represents the approximate solution (3.43) for $g = 133.3$ i.e. $Rg \simeq 42.745$.

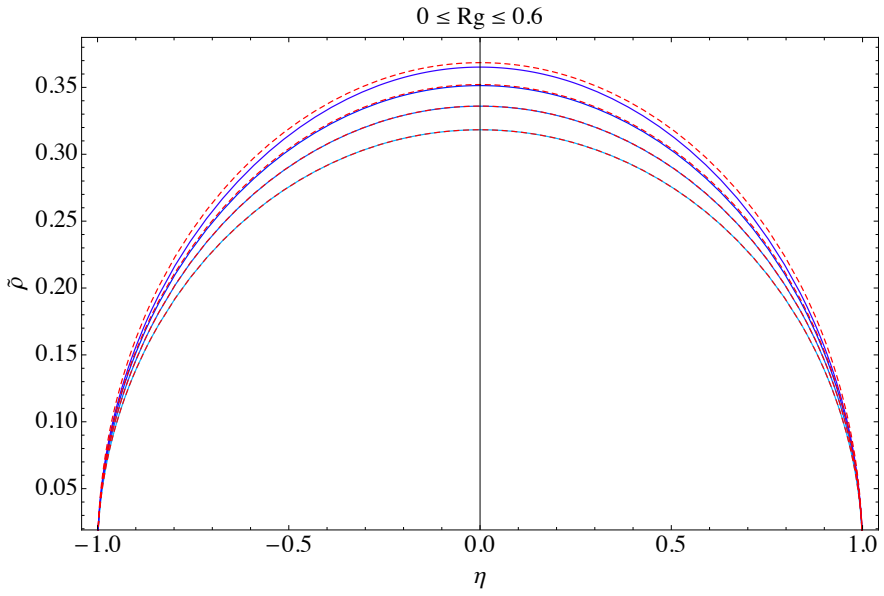

Figure 2. The figure shows the eigenvalue distribution $\rho_1(x)$ for $0 \leq g \leq 0.6$. The dashed red curves represent the approximate solution (3.9) while the blue curve represents the numerical solution for the corresponding value of g. The bottom curve is the Wigner semi-circle $g = 0$.

The blue curves in figure 4 represent the exact results for the radius R and the observ-

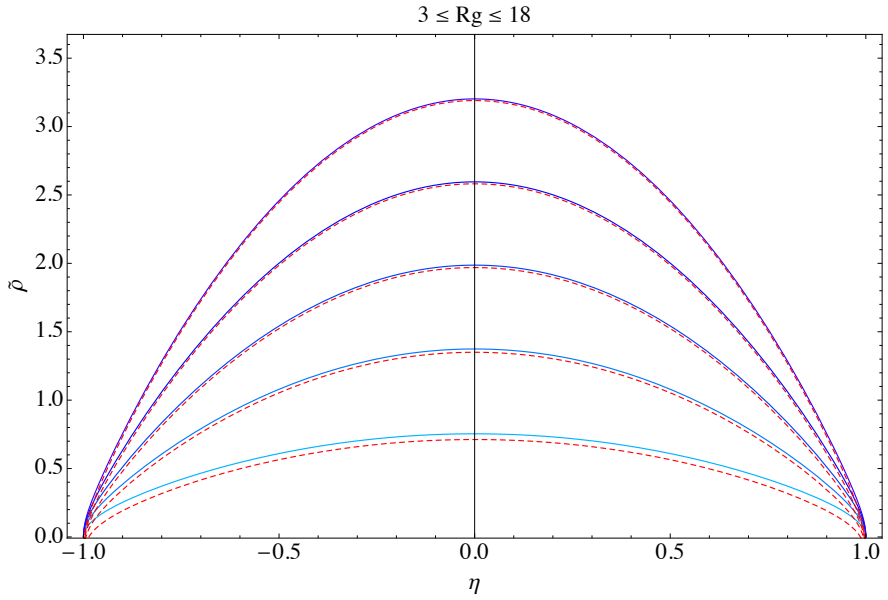

Figure 3. The figure shows $\tilde{\rho}(\eta)$ in the large Rg regime $0 \leq Rg \leq 18$, with the red dashed lined the theoretical expression (3.41) and the blue curves the numerical solution.

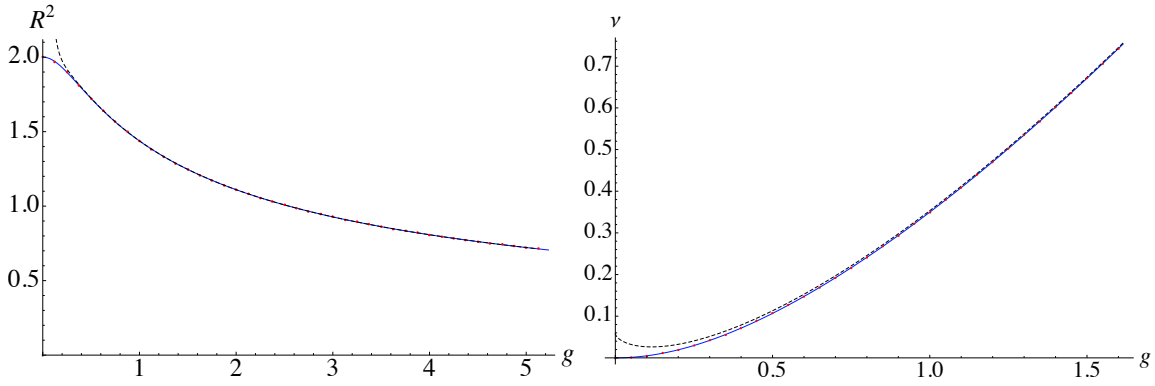

Figure 4. $R(g)$ and $\nu(g)$ The blue curves are the exact results (B.5) and (B.2). The dashed curves are the large g approximate expressions (B.8) and (B.4), while the doted red curves are the numerical solution to (3.44).

able ν given by equations (B.5) and (B.2). The dashed curves are the large g approximate expressions (B.8) and (B.4) one can see that for $g > 1$ there is excellent agreement with the exact result. Finally the doted red curves represent the numerical result obtained by solving numerically the integral equation (3.44). One can observe the perfect agreement of the numerical and the exact results.

4 2D distribution at general coupling

In this section we present our numerical results for the lifted 2D distribution at general coupling. The easiest way to achieve this is to "lift" the distributions of the previous

section. We will describe this in some generality.

4.1 Lifting the distribution and Abel's integral equation

Let us comment on the relation between rotationally invariant distributions in different dimension, which is a generalization of the relation (3.2). Consider a $d-1$-dimensional distribution ρ_{d-1} obtained by reducing a d-dimensional rotationally invariant distribution ρ_d:

$$\rho_{d-1}(r) = \int_{-\sqrt{R^2-r^2}}^{\sqrt{R^2-r^2}} \rho_d(\sqrt{r^2+z^2})dz \ . \tag{4.1}$$

Using the change of variables: $r = \sqrt{R^2-\zeta}$, $z = \sqrt{\zeta-\eta}$ the integral equation can be written as:

$$\rho_{d-1}(\sqrt{R^2-\zeta}) = \int_0^{\zeta} \frac{\rho_d(\sqrt{R^2-\eta})}{\sqrt{\zeta-\eta}} d\eta \ . \tag{4.2}$$

Equation (4.2) is Abel's integral equation with a solution given by [**?**]:

$$\rho_d(w) = \frac{1}{\pi}\frac{d}{d\eta}\int_0^{\eta} \frac{\rho_{d-1}(\sqrt{R^2-t})}{\sqrt{\eta-t}} dt\Big|_{\eta=R^2-w^2} = \frac{1}{\pi\,\omega}\frac{d}{d\omega}\int_R^{\omega} \frac{\rho_{d-1}(r)\,r}{\sqrt{r^2-\omega^2}}\,dr \ . \tag{4.3}$$

It is an easy exercise to obtain the two dimensional distribution corresponding to ρ_1 via equation (4.3). At zero coupling the Wigner semicircle (3.6) corresponds to the a uniform distribution $\rho = \frac{1}{2\pi}$, while at strong coupling the parabolic distribution (3.12) reproduces the hemisphere distribution (2.20). We will use equation (4.3) to "lift" the approximate solution to ρ_1 for general couplings.

4.2 Numerical results

Using equation (4.3) we can "lift" the numerical solution from the previous section for the one dimensional distribution to obtain a two-dimensional rotationally invariant distribution which in the commuting phase of the model coincides with the joint eigenvalue distribution. Furthermore for large coupling, g, we can lift the approximate expression for ρ_1 from equation (3.43). Note that since $|x| \leq R \sim g^{-1/3}$ the second term in equation (3.43) is of order $\log(g)/g^{1/3}$ and dies out at large g. The lift of the first term is part of a semicircle of radius $(3\pi/2)^{1/3}g^{-1/3}$. The lifted distribution at large g is then given by:

$$\rho(x) = \begin{cases} \frac{g}{\pi^2}\left(\left(\frac{3\pi}{2g}\right)^{2/3} - x^2\right)^{1/2} + O\left(\frac{\log g}{g^{1/3}}\right) \ , & \text{for } \ 0 \leq x \leq R \\ 0 \ , & \text{for } \ \mathrm{x > R} \end{cases} \ , \tag{4.4}$$

where R is given by equation (3.36). Note that at the boundary ($x = R$) the distribution is non-zero. Using equation (3.36) one can estimate the magnitude of the distribution at the boundary:

$$\rho(R) = \frac{\sqrt{\log(96\pi^4\,g^2)}}{2^{1/6}3^{1/3}\pi^{7/3}} g^{1/3} + \dots \ , \tag{4.5}$$

which is growing with g. However the magnitude of the maximum of the distribution, at $x = 0$, is $\rho(0) = (3\pi^5/2)^{1/3}\, g^{2/3}$ which grows faster with g. Therefore in the limit $g \to \infty$ the shape of the distribution approaches a hemisphere.

In figure 5 we present our numerical results for the distribution $\rho(x)$ for different coupling constants $0 \leq g \leq 12$. The continuous curves represent our numerical results for

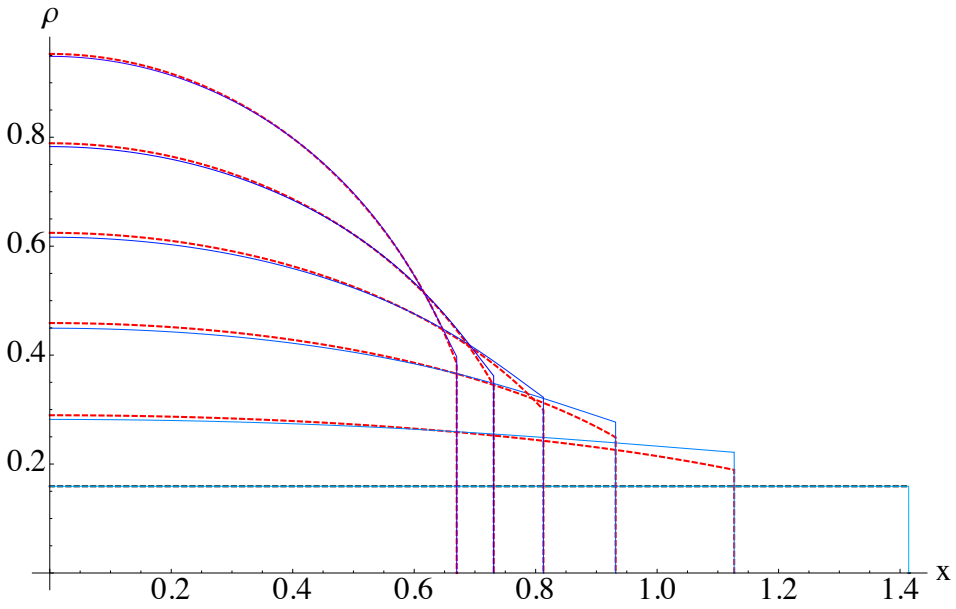

Figure 5. The figure shows the lifted two dimensional distribution as the coupling is increased. The dashed black curve (uniform distribution) is the lift of the Wigner distribution at $g = 0$. The red dashed curves are the approximation (4.4) while the solid curves are the numerical results for the lifted distribution.

the lifted distribution and the colour changes from bright blue to violet as g increases. The black dashed curve represents a uniform distribution of magnitude $1/(2\pi)$, one can see the perfect fit with the numerical results for $g = 0$ (the light blue curve). The red dashed curves represent the approximate expression (4.4) and one can see how the approximation improves as g increases and at $g = 12$ ($Rg \simeq 8$) it is already excellent.

5 Three matrix model realization

Let us now consider the model (also originally introduced parenthetically by Hoppe [11] page 73):

$$\mathcal{Z} = \int \mathcal{D}X\mathcal{D}Y\mathcal{D}Z e^{-N\mathrm{tr}(\mathrm{X}^2+\mathrm{Y}^2+\mathrm{Z}^2-\mathrm{i}\alpha[\mathrm{X},\mathrm{Y}]\mathrm{Z})} \,. \tag{5.1}$$

It is easy to verify that if one integrates out the Z matrix and defines $g^2 = (i\alpha)^2/4$ one recovers the two matrix model (2.1). This suggests that the model (5.1) should be as solvable as the two matrix model. Note also that there is a global $SO(3)$ symmetry rotating the X, Y and Z matrices. In ref. [13] the model (5.1) was analyzed in the spirit

of section 1. Namely the Hermitian matrices X, Y and Z were split into diagonal and off diagonal modes:

$$X_{ij} = x_i^1\delta_{ij}+a_{ij}^1;\;\; Y_{ij} = x_i^2\delta_{ij}+a_{ij}^2;\;\; Z_{ij} = x_i^3\delta_{ij}+a_{ij}^3;\;\; \vec{x}_i = (x_i^1, x_i^2, x^3);\;\; \vec{a}_{ij} = (a_{ij}^1, a_{ij}^2, a_{ij}^3) \tag{5.2}$$

and introduced an axial gauge $\vec{n}.\vec{a} = 0$, where $\vec{n}$ is a three dimensional unit vector. After integrating out the perpendicular degrees of freedom one arrives at the following effective action:

$$S_{\text{eff}}[(\vec{n}.\vec{x})] = \frac{1}{N}\sum_{i=1}^{N}(\vec{n}.\vec{x}_i)^2 - \frac{1}{2N^2}\sum_{i,j=1}^{N}\log\left[\frac{g^2(\vec{n}.(\vec{x}_i-\vec{x}_j))^2}{1+g^2(\vec{n}.(\vec{x}_i-\vec{x}_j))^2}\right] + \frac{(N-1)}{2N}\log g^2 \;. \tag{5.3}$$

Then considering a coarse grained approximation and varying the corresponding distribution function ρ_3 one arrives at the equation:

$$\mu + (\vec{n}.\vec{x})^2 = \int d^3x'\rho_3(\vec{x}')\log\left[\frac{g^2(\vec{n}.(\vec{x}-\vec{x}'))^2}{1+g^2(\vec{n}.(\vec{x}-\vec{x}'))^2}\right] \;. \tag{5.4}$$

Equation (5.4) can be averaged over a unit two-sphere (integrating both sides of the equation by $\frac{1}{4\pi}\int d\Omega_2$) to obtain:

$$\mu + \frac{1}{3}\vec{x}^2 = \int d^3x'\,\rho_3(\vec{x}')\left\{\frac{-2\arctan(g|\vec{x}-\vec{x}'|)}{g|\vec{x}-\vec{x}'|} + \log\left[\frac{g^2(\vec{x}-\vec{x}')^2}{1+g^2(\vec{x}-\vec{x}')^2}\right]\right\} \;. \tag{5.5}$$

Next we apply the Laplacian Δ_x to both side of equation (5.5). The result is:

$$1 = \int d^3x'\,\frac{\rho_3(x')}{|\vec{x}-\vec{x}'|^2(1+g^2|\vec{x}-\vec{x}'|^2)} \;, \tag{5.6}$$

where $x = |\vec{x}|$ and we have used that the lifted distribution ρ_3 is rotationally invariant ($\rho_3(\vec{x}) = \rho_3(x)$). To obtain ρ_3 we need to solve the integral equation (5.6). Integrating over the angular coordinates in (5.6) and multiplying both sides of the equation by x results in:

$$x = \int_0^R dx'\,\pi\,x'\,\rho_3(x')\,\log\left[\frac{(x+x')^2(1+g^2(x-x')^2)}{(x-x')^2(1+g^2(x+x')^2)}\right] \;. \tag{5.7}$$

If we extend the integral in equation (5.7) over an even interval the integral equation can be written as:

$$x = \int_{-R}^{R} dx'\,(-2\pi x'\rho_3(|x'|))\,K_1(g, x'-x) \;, \tag{5.8}$$

where K_1 is the kernel (3.14) from section 3. Comparing equations (5.8) and (3.15) one arrives at the following relation between ρ_1 and ρ_3:

$$\rho_3(x) = -\frac{\rho_1'(x)}{2\pi x} \;, \qquad x > 0 \;. \tag{5.9}$$

In fact equation (5.9) can be proven in more generality. Let us consider a rotationally invariant distribution in d dimensions. The rotationally invariant distribution in $d-2$

dimensions obtained by integrating out two of the spacial dimensions can be obtained by integrating over a disk:

$$\rho_{d-2}(x) = 2\pi \int_0^{\sqrt{R^2-x^2}} \rho_d(\sqrt{x^2+r^2})\, r\, dr = 2\pi \int_x^R \frac{\rho_d(\zeta)}{\zeta}\, d\zeta \ , \tag{5.10}$$

where in the last expression we defined $\zeta = \sqrt{x^2+r^2}$. Now after differentiating the first and the last expressions in (5.10) by x, the integral equation for ρ_d reduces to an algebraic one which can easily be solved to obtain the analogue of equation (5.9):

$$\rho_d(x) = -\frac{\rho'_{d-2}(x)}{2\pi x} \ , \qquad x > 0 \ . \tag{5.11}$$

These considerations confirm that the procedure of averaging over $\vec{n}$ in equation (5.4) is equivalent to lifting the one dimensional distribution (via equation (5.11)).

It is a straightforward exercise to "lift" the results of section 3 to the three dimensional case using equation (5.9):

5.1 3D distribution at weak coupling

At vanishing coupling the Wigner semicircle (3.6) is lifted to:

$$\rho_3(x) = \frac{1}{2\pi^2}\, \frac{1}{\sqrt{2-x^2}} \ , \tag{5.12}$$

which is divergent but integrable at the boundary. In analogy with the one dimensional case where the distribution behaves as $\sqrt{R^2-x^2}$ near the boundary for any finite coupling, equation (5.12) suggests that the lifted three dimensional distribution will diverge as $1/\sqrt{R^2-x^2}$ for any finite coupling g.

To obtain the perturbative expression for ρ_3 at small g it is convenient to change variables $\eta = x/R$ and $\tilde{\rho}_3(\eta) = R\,\rho_3(R\,\eta)$. The lift of equation (3.9) is then given by:

$$\tilde{\rho}_3(\eta) = \frac{1}{\sqrt{1-\eta^2}} \left[\frac{1}{2\pi^2} + \frac{(Rg)^2}{4\pi^2} - \frac{\left(12\eta^2-5\right)(Rg)^4}{16\pi^2} + \frac{\left(40\eta^4+28\eta^2-31\right)(Rg)^6}{32\pi^2} + O\left((Rg)^8\right) \right] . \tag{5.13}$$

5.2 3D distribution at strong coupling

In the limit $g \to \infty$ the one dimensional distribution is parabolic (3.12) with radius (2.21). The lifted three dimensional distribution is uniform (obtained in ref. [13]):

$$\rho_3(x) = \frac{g}{2\pi^2} \quad \text{or} \quad \tilde{\rho}_3(\eta) = \frac{Rg}{2\pi^2} \ . \tag{5.14}$$

Note that since the model is commuting in the limit $g \to \infty$, the lifted distribution in equation (5.14) is also the three dimensional eigenvalue distribution of X, Y, Z.

It is straightforward to lift the correction to the distribution $\Delta\tilde{\rho}$ (3.41) at large but finite g:

$$\tilde{\rho}_3(\eta) = \begin{cases} \frac{Rg}{2\pi^2} + \frac{1}{2\pi^3(1-\eta^2)} - \frac{1}{4\pi^3\eta}\log\left[\frac{1-\eta}{1+\eta}\right] + O\left(\frac{\log(Rg)}{Rg}\right) & \text{if } |\eta| \leq 1-\delta \\ 0 & \text{if } |\eta| \geq 1-\delta \end{cases} \tag{5.15}$$

with $\delta = W(1/e)/(2\pi Rg)$ as in (3.41). Finally we lift the approximate expression for ρ_1 (3.43) to obtain the expression for ρ_3:

$$\rho_3(x) = \frac{g}{2\pi^2} + \frac{1}{2\pi^3}\frac{\left(\frac{3\pi}{2g}\right)^{1/3}}{\left(\frac{3\pi}{2g}\right)^{2/3} - x^2} - \frac{1}{4\pi^3 x}\log\left[\frac{\left(\frac{3\pi}{2g}\right)^{1/3} - x}{\left(\frac{3\pi}{2g}\right)^{1/3} + x}\right] + O\left(\frac{\log g}{g}\right), \tag{5.16}$$

where $x \in (0, R)$ and R is given in equation (2.21).

5.3 3D distribution at general coupling

In this subsection we use equation (5.9) to lift the interpolating solution $\tilde{\rho}$ from section 3.

In figure 5 we present a plot of the numerical solution for the expression $\sqrt{1-\eta^2}\,\tilde{\rho}_3(\eta)$ for $Rg \in [5, 55]$. The color of the curves changes from blue to violet as Rg increases. The red dashed curves represent the approximate expression (5.15) for $\sqrt{1-\eta^2}\,\tilde{\rho}_3(\eta)$. One can see that the approximation improves as one moves far from the boundary $\eta = 1$. One can also observe how the approximation improves as Rg grows.

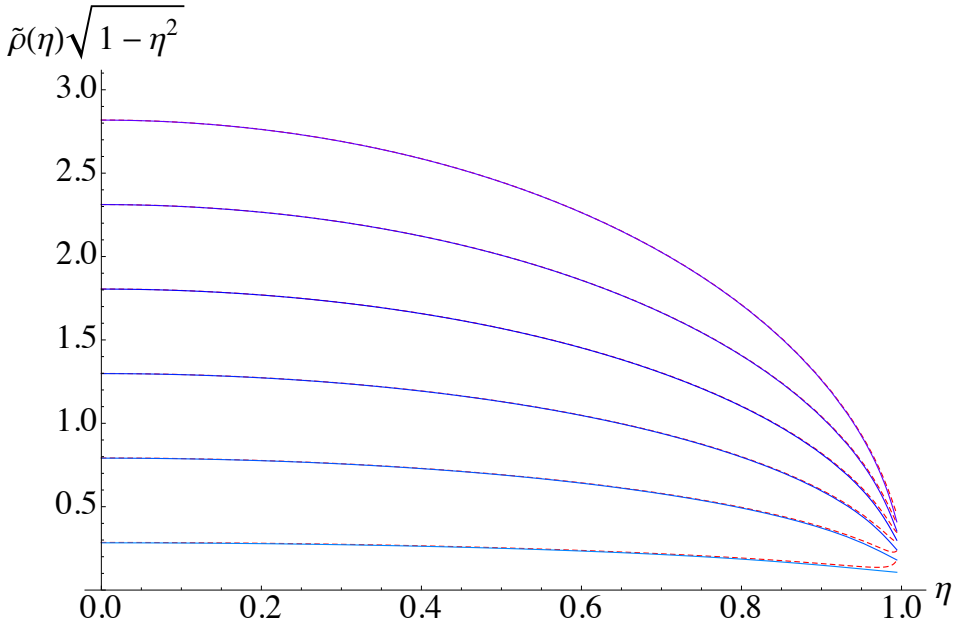

Figure 6. The figure shows the three dimensional rotationally invariant lifted distribution $\tilde{\rho}_3(\eta)$ rescaled by $\sqrt{1-\eta^2}$ for $5 \leq Rg \leq 55$. The continuous curves are the numerical solutions to the integral equation and the dashed red curves are the approximate solution (5.15).

6 Discussion

We have performed a rather detailed study of Hoppe's 2-matrix model (2.1) and in particular developed both perturbative and interpolating solutions for the eigenvalue distribution of either matrix. We "lifted" this one matrix eigenvalue distribution, i.e. the one dimensional distribution, to rotationally invariant distributions in both two and three dimensions. For large couplings these lifted distributions capture the joint eigenvalue distributions of the two and three matrix models.

We found that the two dimensional distribution does not go to zero at the boundary but rather has a finite value, $\rho(R)$, given in (4.5), that grows as $\rho(R) \sim g^{\frac{1}{3}} \ln(g)$ for large g; see Figure 6. This implies that the distribution lifted to a rotationally invariant 3-dimensional distribution must diverge at the boundary for any finite g.

From Figure 6, and the fact that this is the lift of the two dimensional distribution shown in Figure 5, we can deduce that near the boundary the asymptotic behaviour of $\rho_3(x)$ is given by

$$\rho_3(x) \sim \frac{g}{2\pi^2} + \frac{\rho(R)}{\pi\sqrt{(\frac{3\pi}{2g})^{\frac{2}{3}} - x^2}}. \tag{6.1}$$

The divergence[3] of $\rho_3(x)$ as x approaches the boundary is an essential feature as without it the limiting two dimensional distribution could not attain a non-zero value at its boundary. This in turn means that the one dimensional distribution, asymptotically close to the boundary, is given by

$$\rho_1(x) \sim 2\rho(R)\sqrt{R^2 - x^2} \tag{6.2}$$

and the distribution crosses over to a Wigner semicircle as the boundary is approached.

The implication of this is that the noncommutative modes, which of necessity are present in the model, are concentrated near the boundary of the distribution, i.e. they are associated with the largest eigenvalues.

The techniques used in this paper are applicable to a wide variety of models. The large coupling analysis of section 3, taking advantage of the δ-convergent sequence nature of the kernel, is novel and is easily applicable to a wider class of models. Also the interpolation approach of section 3.3, is novel and can be adopted to more general situations.

The models studied here have the important feature that for large couplings the dominant configurations are commuting matrices. The fluctuations around these commuting modes are always present and so the full matrices never truly commute. This is in part reflected in the divergence, as the boundary is approached, of the "lifted" three dimensional distribution. This divergence is subleading for large coupling but an essential feature of such models none the less.

[3] In contrast to the approximation (5.16), which is not integrable at the boundary, the form (6.1) is integrable with the divergence capturing the nature of the distribution in the region $1 - \delta \leq \frac{x}{R} \leq 1$.

7 Acknowledgements

We thank Thomas Kaltenbrunner and Rodrigo Delgadillo-Blando for helpful discussions. The work of V. F. was supported by an INSPIRE IRCSET-Marie Curie International Mobility Fellowship.

A Solving for the hemisphere distribution

In this appendix we solve the integral equation (2.19). Substituting $y(x) = x\rho(x)$ we arrive at:

$$f(x) = -\frac{g}{8}\left(\mu' + \frac{\vec{x}^2}{2}\right) = \int_0^R dx' \frac{y(x')}{x+x'} K\left(\frac{2\sqrt{xx'}}{x+x'}\right) \ , \tag{A.1}$$

The solution to equation (A.1) is given by [14, 15]:

$$y(x) = -\frac{4}{\pi^2}\frac{d}{dx}\int_x^R \frac{t\,F(t)\,dt}{\sqrt{t^2-x^2}} \ , \quad F(t) = \frac{d}{dt}\int_0^t \frac{s\,f(s)\,ds}{\sqrt{t^2-s^2}} \ . \tag{A.2}$$

Substituting $f(x)$ from equation (A.1) into equation (A.2) we obtain:

$$y(x) = x\,\frac{g}{\pi^2}\,\frac{\frac{R^2-\mu'}{2} - x^2}{\sqrt{R^2-x^2}} \ , \tag{A.3}$$

which implies equation (2.20).

B Exact Results

In this appendix we provide with slight extension some of the exact results for the model (2.1) obtained in ref. [6]. One of the exact results of the authors of ref. [6] was a closed form expression for the observable:

$$\nu = g^2 \int_{-R}^{R} dx\,\rho_1(x) \ . \tag{B.1}$$

It is given by:

$$\nu(m) = \frac{1}{12} - \frac{K^2}{5\pi^2}\frac{10\vartheta^2(\vartheta+m-2) + 2\vartheta(6-6m+m^2) + (1-m)(m-2)}{3\vartheta^2 + 2(m-2)\vartheta + 1 - m} \ , \tag{B.2}$$

where $K = K(m)$ and $\vartheta = E(m)/K(m)$ (E and K are the standard elliptic integrals). The elliptic modulus m can be determined in terms of the coupling constant g via:

$$g^2(m) = \frac{K^4}{3\pi^4}\left(-3\vartheta^2 + 2(2-m)\vartheta - (1-m)\right) \ . \tag{B.3}$$

Equations (B.2) and (B.3) specify (in parametric form) the g dependence of the observable ν. For large g one can obtain the expansion:

$$\nu = \frac{(12\pi)^{2/3}}{20} g^{4/3} - \frac{3}{(12\pi)^{2/3}} g^{2/3} + \left(\frac{1}{12} - \frac{1}{4\pi^2}\right) + O(g^{-2/3}) \ . \tag{B.4}$$

Another exact result obtained in ref. [6] relevant to our discussion is the radius of the distribution R for which the authors derived the following integral presentation:

$$R = \frac{1}{2} \int_{x_4}^{x_3} dt \, \frac{x_3 - t}{\sqrt{(x_2 - t)(x_1 - t)(t - x_4)}} \ , \tag{B.5}$$

where x_1, x_2, x_3 and x_4 are functions of m given by:

$$\begin{aligned} x_1 &= \frac{K^2}{g^2\pi^2}(2 - m - 2\vartheta); \quad x_2 = \frac{K^2}{g^2\pi^2}(1 - 2\vartheta); \\ x_3 &= \frac{K^2}{g^2\pi^2}(3\vartheta + m - 2); \quad x_4 = \frac{K^2}{g^2\pi^2}(1 - m - 2\vartheta); \ . \end{aligned} \tag{B.6}$$

The integral (B.5) can be solved in closed form:

$$R(m) = \frac{K(m)}{\pi\, g(m)} Z(\sin^{-1} \sqrt{\frac{1 - \vartheta(m)}{m}} \,|\, m) \ , \tag{B.7}$$

where $Z(\phi \,|\, m)$ is the standard Jacobi Zeta function. To obtain a large g expansion of R we expand equation (B.7) near $m = 1$. Using equation (B.3) we can obtain the expansion used in equation (3.36):

$$R = \left(\frac{3\pi}{2}\right)^{1/3} g^{-1/3} - \frac{2\log\, g + \log(96\pi^4)}{6\pi} g^{-1} + \frac{1}{2^{8/3}3^{1/3}\pi^{7/3}} g^{-5/3} + O(g^{-7/3}) \ . \tag{B.8}$$

References

[1] R. Dijkgraaf, E. P. Verlinde and H. L. Verlinde, "Matrix string theory," Nucl. Phys. B **500** (1997) 43 [hep-th/9703030].

[2] N. Ishibashi, H. Kawai, Y. Kitazawa and A. Tsuchiya, "A Large N reduced model as superstring," Nucl. Phys. B **498** (1997) 467 [hep-th/9612115].

[3] A. Connes, M. R. Douglas and A. S. Schwarz, "Noncommutative geometry and matrix theory: Compactification on tori," JHEP **9802** (1998) 003 [hep-th/9711162].

[4] T. Banks, W. Fischler, S. H. Shenker and L. Susskind, "M theory as a matrix model: A Conjecture," Phys. Rev. D **55** (1997) 5112 [hep-th/9610043].

[5] D. E. Berenstein, J. M. Maldacena and H. S. Nastase, "Strings in flat space and pp waves from N=4 Super Yang Mills," AIP Conf. Proc. **646** (2003) 3.

[6] V. A. Kazakov, I. K. Kostov and N. A. Nekrasov, "D-particles, matrix integrals and KP hierarchy," Nucl. Phys. B **557**, 413 (1999) [arXiv:hep-th/9810035].

[7] R. Delgadillo-Blando, D. O'Connor and B. Ydri, "Geometry in Transition: A Model of Emergent Geometry," Phys. Rev. Lett. **100** (2008) 201601 [arXiv:0712.3011 [hep-th]].

[8] R. Delgadillo-Blando and D. O'Connor, "Matrix geometries and Matrix Models," JHEP **1211** (2012) 057 [arXiv:1203.6901 [hep-th]].

[9] H. Steinacker, "Gravity and compactified branes in matrix models," JHEP **1207** (2012) 156 [arXiv:1202.6306 [hep-th]].

[10] D. N. Blaschke and H. Steinacker, "Schwarzschild Geometry Emerging from Matrix Models," Class. Quant. Grav. **27** (2010) 185020 [arXiv:1005.0499 [hep-th]].

[11] Hoppe, J. R. 1982, Ph.D. Thesis.

[12] D. E. Berenstein, M. Hanada and S. A. Hartnoll, "Multi-matrix models and emergent geometry," JHEP **0902**, 010 (2009) [arXiv:0805.4658 [hep-th]].

[13] D. O'Connor and V. G. Filev, "Near commuting multi-matrix models," arXiv:1212.4818 [hep-th].

[14] Polyanin,A. D.,Manzhirov, A. V. ,Handbook of Integral Equations: Second Edition, 2008

[15] Zabreyko, P. P., Koshelev, A. I., et al., Integral Equations: A Reference Text, Noordhoff Int. Publ., Leyden, 1975.